International Journal of High-Rise Buildings
June 2014, Vol 3, No 2, 107-120

International Journal of
High-Rise Buildings
www.ctbuh-korea.org/ijhrb/index.php

Strength Demand of Hysteretic Energy Dissipating Devices Alternative to Coupling Beams in High-Rise Buildings

Kyung-Suk Choi and Hyung-Joon Kim†

University of Seoul, Siripdae-gil 163, Dongdaemun-gu, Seoul 130-743, Korea

Abstract

A Reinforced concrete (RC) shear wall system with coupling beams has been known as one of the most promising structural systems for high-rise buildings. However, significantly large flexural and/or shear stress demands induced in the coupling beams require special reinforcement details to avoid their undesirable brittle failure. In order to solve this problem, one of promising candidates is frictional hysteretic energy dissipating devices (HEDDs) as an alternative to the coupling beams. The introduction of frictional HEDDs into a RC shear wall system increases energy dissipation capacity and maintains the frame action after their yielding. This paper investigates the strength demands (specifically yield strength levels) with a maximum allowable ductility of frictional HEDDs based on comparative non-linear time-history analyses of a prototype RC shear wall system with traditional RC coupling beams and frictional HEDDs. Analysis results show that the RC shear wall systems coupled by frictional HEDDs with more than 50% yield strength of the RC coupling beams present better seismic performance compared to the RC shear wall systems with traditional RC coupling beams. This is due to the increased seismic energy dissipation capacity of the frictional HEDD. Also, it is found from the analysis results that the maximum allowable ductility demand of a frictional HEDD should increase as its yield strength decreases.

Keywords: RC shear walls, Strength demand, Hysteretic Energy Dissipating Devices (HEDDs), Coupling beams, Frame action

1. Introduction

A Reinforced concrete (RC) shear wall system has been known as one of most promising structural systems for high-rise buildings due to its high stiffness and strength structural characteristics. In RC shear wall systems, coupling beams are usually used to connect RC shear walls to further increase stiffness and strength of a high-rise building. Also, coupling beams increase structural redundancy compared to cantilever type RC shear walls. However, significantly large flexural and/or shear stress demands are applied to coupling beams because of the large rigidity induced from RC shear walls. This is more true for coupling beams in high-rise buildings with coupled RC shear walls. Especially, coupling beams with low span-depth ratios become shear-critical members which are expected to suffer brittle failure. Special reinforcement details are generally required to avoid the undesirable brittle failure of such coupling beams (Paulay and Binney, 1974; Paulay and Santhakumar, 1976; Harries, 2000). Engineering and economic efforts need to utilize special reinforcement details in the coupling beams.

In order to figure out the problem regarding complicated reinforcement details of the coupling beams in RC shear wall structural systems, various methods have been suggested and verified analytically and experimentally (Harries et al., 1998; Kim et al., 2012; Chung et al., 2009). One of promising candidates for alternative to ductile coupling beams with special reinforcement details is hysteretic energy dissipating devices (HEDDs). The introduction of HEDDs into RC shear wall systems increases seismic input energy dissipation capacity and maintains the frame action after their yielding. They have been increasingly applied for building structures to reduce their seismic demands, such as accelerations, velocities, displacement, etc. and in turn to decrease structural and non-structural damage which could occur during strong ground motion. Of various mechanisms applicable to energy dissipating devices, HEDDs typically utilize friction mechanism and steel plastic behavior to dissipating seismic input energy (Christopoulos et al., 2006; Tremblay et al., 2014). Fig. 1 shows a HEDD that uses the rotational friction behavior of specially designed friction interface consisting of brake-lining pads and stainless steel sheet. Also, presented in the figure is experimental evidence showing the very stable friction cyclic response without any stiffness and strength degradation. These HEDDs can be modeled using elements following the bilinear elasto-plastic hysteresis rule.

In the design of frictional HEDDs for applications to a RC shear wall system, three structural characteristics of the HEDDs, their stiffness, yield strength, and maximum allowable ductility, shall be determined in the design stage

†Corresponding author: Hyung-Joon Kim
Tel: +82-2-6490-2763; Fax: +82-2-6490-2749
E-mail: hyungjoonkim@uos.ac.kr

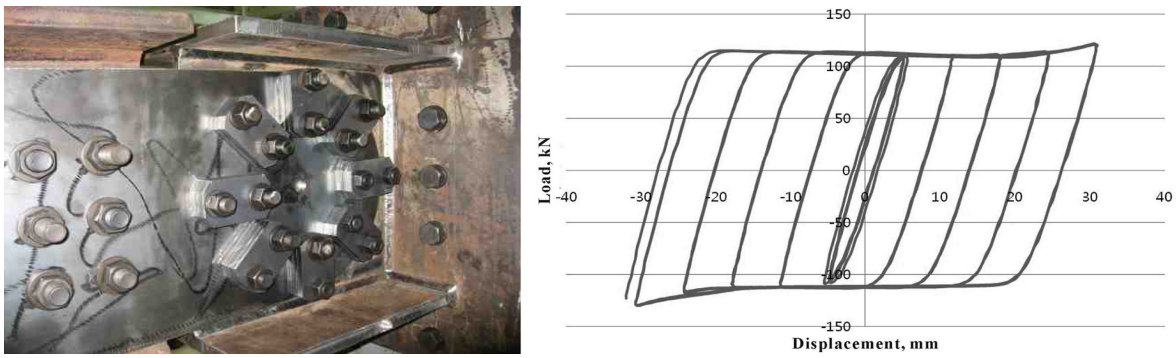


Figure 1. Shape and experimental cyclic response of frictional HEDDs.

of a building. Of the three structural characteristics, the stiffness of a HEDD is mainly dependent on that of the connection components with the frictional HEDD so that it can be easily designed to have the same stiffness of a corresponding coupling beam because the frictional HEDD itself has infinite stiffness, as mentioned earlier. From this point of view, it is a remaining issue for the design HEDD to determine the yield (sliding) force and maximum allowable ductility that achieve better (or equivalent) seismic performance than (or to) traditional RC shear wall systems connected with coupling beams.

This paper investigates the yield strength levels with a maximum allowable ductility required to frictional HEDDs that are used for alternative to coupling beams connecting RC shear walls. To do this, this paper first describes the expected cyclic behavior of RC shear walls coupled with HEDDs compared to that of traditional RC shear walls with RC coupling beams. A 30-story building is chosen as a prototype building of which the seismic-force-resisting system (SFRS) is a RC shear wall system with coupling beams. The SFRS is first designed according to current Korean Seismic Design Code (KBC, 2009). Based on the seismically designed prototype SFRS, coupling beams are replaced with frictional HEDDs with different yield strengths (sliding forces). For non-linear time-history analysis of the prototype building, their analytical models are developed. Analysis results are discussed in terms of maximum story drifts and energy dissipation. The seismic performance of the prototype RC shear wall systems with coupling beams is compared with that of the RC shear walls connected with frictional HEDDs. Throughout comparative seismic performance, this paper suggests the yield strength levels of frictional HEDDs with the maximum allowable ductility capacities that can achieve the similar or excellent seismic performance to the traditional RC shear wall systems with coupling beams.

2. Structural Behavior of RC Shear Walls Coupled with Frictional Hysteretic Energy Dissipating Devices

Before comparative non-linear time-history analyses of RC shear walls connected by coupling beams or frictional HEDDs, the differences between their structural behaviors are described in this chapter. Fig. 2(a) presents the lateral-force-resisting mechanism of a traditional RC shear wall system before the yielding of coupled beams. The moment, M induced by lateral loads is carried by the flexural resistances of RC shear walls and the coupling moment resulting from the frame action, and is evaluated from (Paulay and Priestly, 1992):

$$M = M_{1,ini} + M_{2,ini} + Tl \tag{1}$$

where $M_{1,ini}$ and $M_{2,ini}$ are respectively, the moments carried by left and right side RC shear walls, T is the tensional reaction of the left-side RC shear wall and equals to the compressional reaction of the right-side RC wall, and l is the distance between the center lines of the RC shear walls. The last term in the right side of Eq. (1) considers the frame action induced by coupling beams connecting RC shear walls.

Recent seismic design philosophy requires the occurrence of plastic hinges at the wall bases that is the main seismic energy dissipating mechanism of a RC shear wall system with coupling beams. However, the plastic hinges at the wall bases generally occur after the yielding of coupling beams. Once stiffness and strength degradation starts to occur in traditional RC coupling beams, the decrease in the flexural resistance resulting from the frame action initiates. The RC shear walls themselves shall resist additional moments to compensate the loss of flexural resistance induced by the RC coupling beams. If all RC coupling beams are totally failed without their residual strengths, as shown in Fig. 2(b), the lateral-force-carrying system becomes two cantilever RC shear walls and Eq. (1) becomes:

$$M = M_{1,cw} + M_{2,cw} \tag{2}$$

where $M_{1,cw}$ and $M_{2,cw}$ are, respectively, the moments carried by left and right cantilever RC shear walls. This means that flexural moment demands resulting from lateral loads depend on only flexural capacities of two canti-

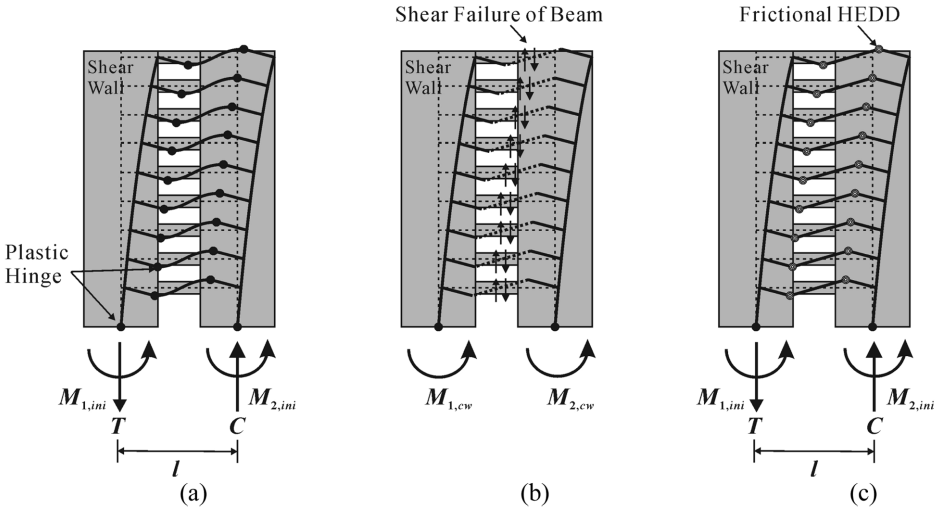


Figure 2. Lateral load-carrying-mechanisms of RC shear wall systems.

lever RC shear walls.

From the comparison between Eqs. (1) and (2), coupling beams are important to increase the lateral stiffness and strength of the RC shear wall system. When a RC shear wall system is subjected to strong ground motion and the plastic hinges occur at the RC shear wall bases, it is not practically possible for coupling beams to be in elastic considering their general sizing. In order to figure out the problems as illustrated in Fig. 2(b), the stiffness and strength degradation of the coupling beams should be prevented even if relatively large shear and/or flexural deformations are imposed to them. For this reason, this study proposes frictional HEDDs as an alternative to coupling beams with complicate special details. Fig. 2(c) shows the lateral load-carrying mechanism of the RC shear wall system with frictional HEDDs which is similar to the mechanism shown in Fig. 2(a) although the components connecting two RC shear walls suffer significant large flexural deformations. Under the assumption that the frictional HEDDs behave elasto-perfect plastic without stiffness and strength degradation, the last term (the lateral-load-carrying capacity resulting from the frame action) in the right side of Eq. (1) is maintained. This means that the RC shear wall system provides the stable lateral-load-carrying resistance before the strength degradation of the RC shear walls occurs due to excessive lateral deformations.

3. Seismic Design and Analytical Models of Studied Frames

3.1. Seismic design of studied frames

Fig. 3 shows the typical rectangular-shaped plane (42 m × 30 m) of a 30-story building that is selected as a prototype high-rise building for this study. The height of the 30-story building is 96 m with a story height of 3.2 m. The seismic-force-resisting systems located at the central part of the building are, respectively, only a RC shear wall system in the *Y*-direction and a RC shear wall systems with coupling beams in the *X*-direction. This study selects the *X*-directional RC shear wall system as a studied frame. The RC shear walls and the RC coupling beams are first designed according to the Korean seismic code (KBC, 2009) and its coupling beams are then replaced with frictional HEDDs with different yield strength levels. Perimeter columns were designed to carry only gravity loads such as dead and live loads. Flat-plate slabs are used for a floor system and post-tensioning technologies are applied to the floor system to remove beam members.

The prototype building is assumed to be located at Song-do which is a northern west part of Korea. The site class is assigned to S_D soil condition. In accordance with KBC2009, The S_D soil is defined as stiff soil that is equal to Site Class D in ASCE/SEI 7 (ASCE, 2010). Its RC shear walls should be satisfied with the design criteria for RC special shear wall systems since the prototype building is categorized into a seismic design category of D. KBC2009 prohibits the construction of ordinary RC shear wall systems of which the seismic design category is D

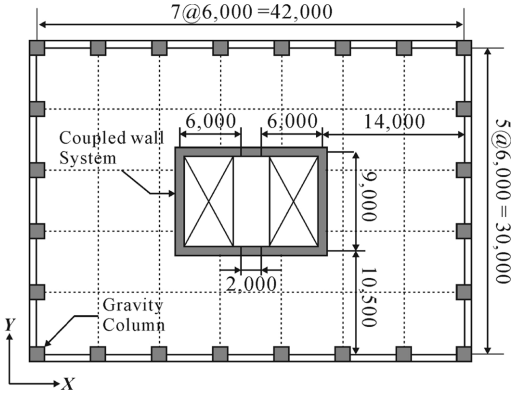


Figure 3. Typical floor plan of the prototype building.

Table 1. Elastic acceleration response spectrum and seismic design parameters

F_a	F_v	S_{DS}	S_{D1}	R	Cd	Ωo	I
1.44	2.09	0.425	0.246	6	2.5	5	1.2

and the height is more than 60 m. This is different with the height limitation of 160 ft prescribed in ASCE/SEI 7. Dead and live loads imposed on the floors are, respectively, 9.7 kN/m^2 and 2.0 kN/m^2. Total seismic weight of the building is assumed to be 413,164 kN that is equal to 100% of dead loads.

Table 1 summarizes the short and 1s-period design spectral accelerations and seismic design factors, such as a response modification factor R, a deflection amplification factor C_d and an overstrength factor Ω_o for the special shear wall systems, and important factor I which is dependent on the seismic hazard level at the building site and an occupation category. The fundamental period empirically estimated using the building height of 96 m and the seismic-force-resisting system is 2.24 sec. A base shear-force of 9,099 kN is calculated by the equivalent lateral force (ELF) method although it is not allowed for the seismic design of the prototype building.

The seismic design of the prototype RC special shear wall system with coupling beams is carried out using a response spectrum analysis (RSA) procedure. Fig. 4 includes structural cross-section of RC shear walls and coupling beams. Concrete with a nominal compressive strength of 24 MPa is used for both RC shear walls and coupling beams. Thicknesses of the studied RC shear walls in the x-direction are varied along with stories: 700 mm for 1st and 2nd stories, 600 mm for 3rd and 8th stories, 500 mm for 9th to 12th stories, 400 mm for 13th to 16th stories, and 300 mm for the other stories. The widths of coupling beams are the same as the thicknesses of RC shear walls connected with them and their height is set to 700 mm based on the opening size. Reinforcements with the tensile strength of 500 MPa and 600 MPa are, respectively, used for the RC shear walls and the coupling beams. Reinforcement details of different sections are also found in the figure. In order to satisfy the design criteria for ductile cyclic response of RC shear walls, special boundary elements are designed in the compressive zone. The coupling beams are designed as flexural structural members according to the requirements of KBC 2009. Neverthe-

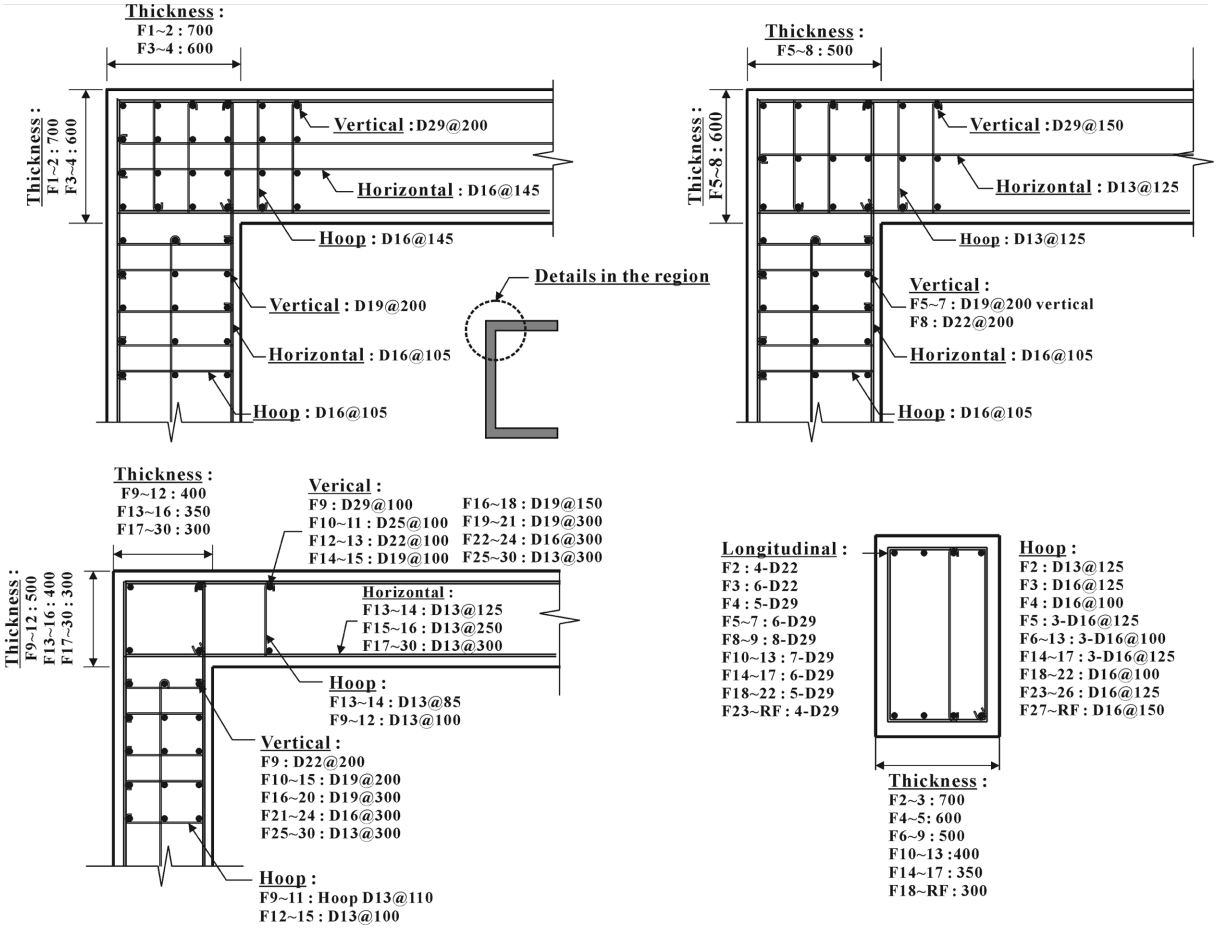


Figure 4. Reinforcement details of RC shear walls and coupling beams.

Table 2. Dynamic characteristics of studied building

Mode	1	2	3	4	5	6	7
Period (sec)	3.05	0.79	0.38	0.23	0.16	0.12	0.09
Modal Participation Mass (%)	60.6	20	6.6	3.6	2.2	1.5	1.1

less, the design of the coupling beams with the span-to-depth ratio of 2.86 is governed by shear force demands so that additional hoops are sized.

Table 2 shows the structural periods and the accumulative mass participation percentages which are obtained from Eigenvalue analysis of the studied frame. The fundamental structural period of 3.05 sec is longer than the period calculated from the empirical equation mentioned earlier. The accumulative mass participation percentage up to the 4th mode is above 90% so that the contribution from 1st to 4th modes is considered in the seismic design of the prototype RC shear wall systems. A base shear of 6,545 kN computed from the modal analysis is smaller than 85% of the base shear obtained from the ELF method that is used for the design base shear of the studied frame according to the code's requirements and conservative design approach.

3.2. Analysis model of studied frames

The seismic performance of the studied frames is evaluated by nonlinear time-history analyses using RUAUMOKO-2D (Carr, 2010). Fig. 5 shows analysis models for the RC shear walls with coupling beams or frictional HEDDs. The 2-D analysis models consist of nonlinear hysteretic elements representing shear walls, coupling beams and frictional HEDDs, and rigid links which is used for connecting between a shear wall and coupling beams or frictional HEDDs (Bolvin and Patrick, 2010). A length of the rigid links is the distance from the center of the shear wall to the end of the coupling beam. Lumped masses are mounted on the nodes in the elements representing the RC shear walls. Relative horizontal displacements of all nodes on the same height are neglected under the assumption that RC slabs have enough thickness to develop diaphragm effects.

The RC shear walls in the analysis models are modeled using General Quadratic BEAM-COLUMN elements in RUAUMOKO-2D. The initial flexural stiffness of the elements is assumed as $0.7E_cI_g$ where E_c is the elastic modulus of concrete and I_g is the moment of inertia for gross section. These elements are capable of capturing the non-symmetric axial force-moment interaction response of the

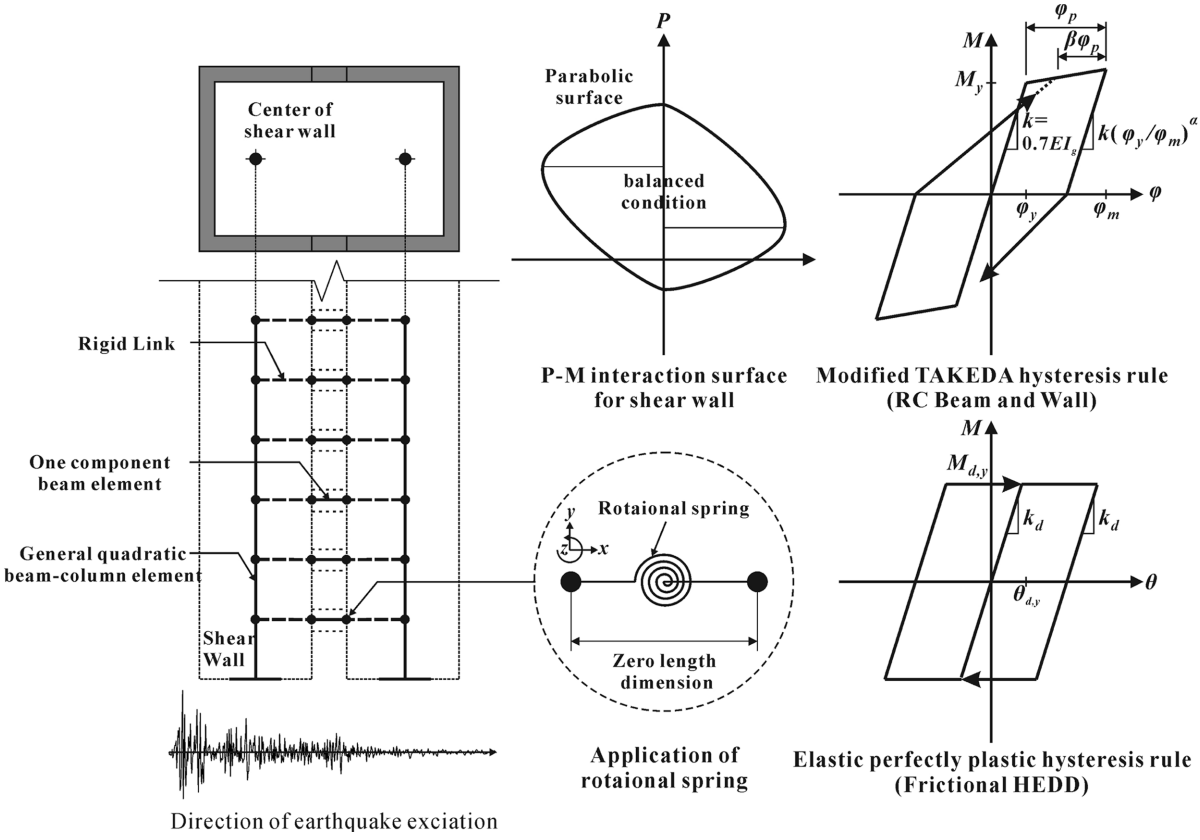


Figure 5. Analysis model of RC shear walls with coupling beams and frictional HEDDs.

C-shaped cross-section structural members like the RC shear walls shown in Fig. 3. The axial force-moment interaction curves of the C-shaped RC shear walls, as shown in Fig. 5, are obtained from RESPONSE 2000 (Collins and Mitchell, 1987). In calculating their axial and flexural strengths, the effects of confined concrete are important. This study uses the Mander's model which can reflect the influence of hoop's geometry on the compressive stress-strain relation of confined concrete (Mander et al., 1988). The elements representing coupling beams are modeled with similar modeling strategies applied to those of RC shear walls, except that One-Component elements are used instead of General Quadratic BEAM-COLUMN elements. One-Component elements are suitable for structural members, such as coupling beams of which axial forces can be negligible. The hysteresis of the RC shear walls and the coupling beams in the studied frame follows the Modified Takeda hysteretic rule (Otani, 1974) which can capture pinching phenomenon and stiffness degradation along with ductility.

In this hysteretic model, values of 0.2 and 0.4 are, respectively, used for ALPHA and BETA which are the stiffness reduction factors in unloading and reloading. The typical Modified Takeda hysteretic rule of the shear walls and the coupling beams is illustrated in Fig. 5. The analysis models for the structural members include strength degradation of which the rule depends on their ductility according to FEMA 356 (FEMA, 2000). For the element of a RC shear wall that can be assumed to be a flexural structural member, its plastic hinge rotation is based on the plastic hinge length, l_{wp} calculated from (Priestly and Kowalsky, 2000):

$$l_{wp} = 0.2L_w + 0.44H_w \tag{3}$$

where L_w and H_w are, respectively, the length and height of a shear wall. On the other hand, the plastic hinge length of a coupling beam is assumed to be a half of its depth. Table 3 summarizes the flexural moments and curvatures, at the yielding, the post-yielding stiffness

Table 3. Nonlinear Properties of the coupling beams

Floor Level	Yielding moment, M_y (kNm)	Yielding Curvature, φ_y (rad/km)	Curvature Ductility	Residual strength ratio
RF	654	9.77	1.20	0.6
30	654	9.77	1.20	0.6
29	654	9.77	1.20	0.6
28	654	9.77	1.20	0.6
27	654	9.77	1.20	0.6
26	654	9.77	1.20	0.6
25	654	9.77	1.20	0.6
24	654	9.77	1.20	0.6
23	654	9.77	1.20	0.6
22	828	12.36	1.16	0.6
21	828	12.36	1.16	0.6
20	828	12.36	1.16	0.6
19	828	12.36	1.16	0.6
18	828	12.36	1.16	0.6
17	959	12.29	1.16	0.6
16	959	12.29	1.16	0.6
15	959	12.29	1.16	0.6
14	959	12.29	1.16	0.6
13	1098	12.30	1.16	0.6
12	1098	12.30	1.16	0.6
11	1098	12.30	1.16	0.6
10	1098	12.30	1.16	0.6
9	1299	11.64	1.17	0.6
8	1299	11.64	1.17	0.6
7	990	8.87	1.22	0.6
6	990	8.87	1.22	0.6
5	1084	8.10	1.25	0.6
4	897	6.70	1.30	0.6
3	684	4.38	1.46	0.6
2	460	2.94	1.68	0.6

ratios, and the ultimate ductility of the coupling beams. From the table, the elements representing the coupling beams are modeled with very limited ductility capacities before strength degradation and with sudden strength losses after the ultimate strengths.

Elasto-perfect plastic (EP) elements shown in Fig. 5 are used for frictional HEDDs that are alternatives to RC coupling beams. The yield strengths of the elements represent the forces at the initiation of rotational sliding occurred at the friction interface. Since the study assumes that the connection members of frictional HEDDs are designed to have the same stiffness as the RC coupling beams, EP elements with zero-length are added at the both ends of the RC coupling beams. The yield strengths of added EP elements are varied to the prescribed values of γ defined as the ratios of their yield strength to the yield strengths of the corresponding RC coupling beams. The values of γ are equal to and smaller than 1.0, which the plastic behavior of the connection elements with the frictional HEDDs is prevented to concentrate structural damage on the frictional HEDDs. Also, the connection element of a frictional HEDD are designed to elastically behave against a shear force demand V_{cu} calculated from:

$$V_{cu} = \frac{2\gamma M_{y,H}}{l_b} \tag{4}$$

where $M_{y,H}$ is the yield strength of the frictional HEDD and l_b is the net length of a corresponding RC coupling beam. Unlike the RC shear walls and coupling beams, strength degradation in the analysis models representing the frictional HEDDs is not considered since they have experimentally sufficient rotational deformation capacities.

4. Comparative Seismic Performance of Studied Frames

For nonlinear time-history analyses of the studied frames, a total of 20 acceleration ground motion records is used and are obtained from10 historical earthquakes (two records for a single historical earthquake). It is noted that the 20 records are originally selected from the data set which was chosen to evaluate the seismic design parameters of seismic-force-resisting systems of FEMA P-695 (FEMA, 2008). Table 4 summarizes the characteristics of the selected earthquake records. The records are scaled to match with the design spectrum of the studied frames. Also, Fig. 6 presents elastic acceleration response spectrum of each scaled record and mean elastic acceleration response spectrum with the design spectrum for direct comparison.

In order to obtain stable analysis results, a Newmark-Beta method is chosen as a computation algorithm and analyses are carried out with the time-spacing of 0.001 sec which is sufficiently smaller than the time-spacing of earthquake records. The initial stiffness Rayleigh damping model with 5% critical is used as an inherent damping model for nonlinear time-history analysis of the studied frames (Chopra, 2001).

4.1. Seismic performance of a RC shear wall system with RC coupling beams

The floor-specific distribution of story drift ratios and average values for 20 earthquakes to the studied frames has been shown in Fig. 7(a). Averages have been presented with bolded solid lines in the figure. From the distri-

Table 4. Properties of ground motion records

Label	Record	Magnitude	Distance(kM)	PGA (g)
EQ01	Northridge, 1994	6.7	13.3	0.416
EQ02	Mulhol			0.516
EQ03	Duzce, 1999	7.1	41.3	0.728
EQ04				0.822
EQ05	Imperial Valley, 1979	6.5	33.7	0.238
EQ06	Delta			0.351
EQ07	Kobe, 1995	6.9	8.7	0.509
EQ08	Nishi-Akashi			0.503
EQ09	Kocaeli, 1999	7.5	98.2	0.312
EQ10	Duzce			0.358
EQ11	Landers, 1992	7.3	86	0.245
EQ12	Yermo			0.152
EQ13	Loma Prieta, 1989	6.9	289	0.529
EQ14	Capitola			0.443
EQ15	Superstition, 1987	6.5	35.8	0.358
EQ16	El Centro			0.258
EQ17	Cape Mendocino, 1992	7	312	0.385
EQ18				0.549
EQ19	San Fernando, 1971	6.6	316	0.210
EQ20				0.174

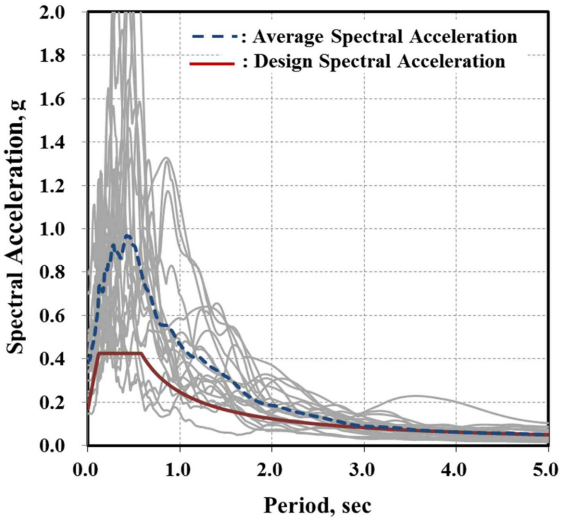
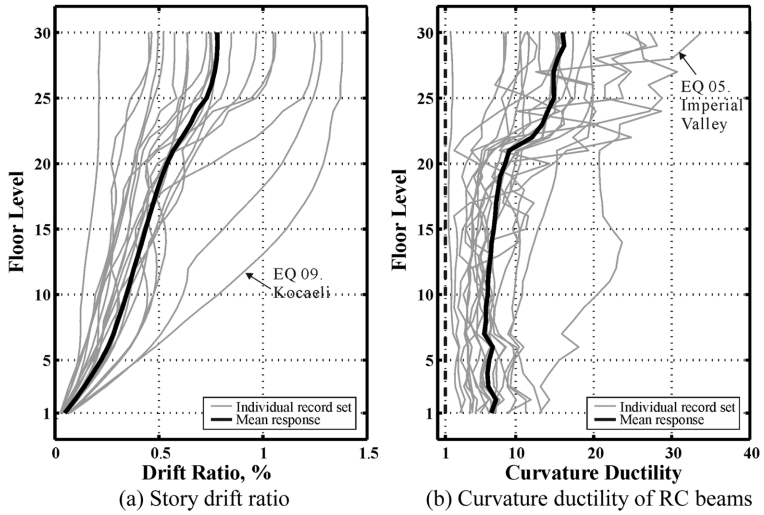


Figure 6. Maximum story drift ratio and curvature ductility of RC beams.

bution of average story drift ratios along with stories, story drift demands increase as stories are higher. This is common seismic response observed in general cantilever-type shear wall structures which is governed by the bending deformation. The average maximum story drift ratio is 0.78%, and large variance of the story drift ratios is measured at higher stories. Some analysis results show the tendency that the story drift ratio decreases around the intermediate stories and then increases again, which is due to the large effect of higher modes. Among the responses of individual seismic waves, the EQ09 Kocaeli earthquake ground motion develops the maximum story drift ratio of 1.38% at the roof floor. The maximum story drift ratio of 1.38% is still less than the value of 1.5% which is specified the allowable story drift ratio for structures in KBC2009. It is witnessed from this observation that the seismic design of the studied frame is properly carried out according to KBC2009.

Fig. 7(b) shows the distribution of maximum curvature ductility and average values of the RC coupling beams at each story for 20 earthquakes. The average maximum curvature ductility has the value of more than 6.0 at all stories and 16.2 at the roof floor. As shown in Table 3, it can be determined that the strength and stiffness of the RC beam have been reduced as its modeling ductility is 1.2 to 1.7. Since a value of 0.6 is, in this study, used as the residual strength ratio (defined as residual strength / yield strength), the RC coupling beams have a certain level of load resistance capacities even after strength reduction has occurred. However, it is known that the RC coupling beams destructed by shear actually shows rapid deterioration, and lose their lateral-load-carrying capacity as structural elements after strength reduction. Therefore, it is expected that the studied frame would lose its lateral-load-resistance imposed by the frame action due to the destruction of the RC coupling beams, and behave as a shear wall system with the two separated cantilever RC shear walls in the event of an actual earthquake. From the distribution of maximum curvature ductilities along with stories, it can be confirmed that the RC coupling beams at 2 to 22 stories have relatively constant level of ductility, but ductilities of the RC coupling beams at the other stories increase. The maximum curvature ductility demand of 35 is found in the RC coupling beams at the roof story when the EQ05 Imperial valley ground motion is subjected.

Fig. 8 shows the analysis results of the studied frames subjected to the EQ09 Kocaeli earthquake record which generates the maximum seismic story drift response. The left figure presents the distribution of plastic hinges, where black circles indicate the plastic hinges accompanied with strength reduction and black half-circles illustrates the plastic hinges without strength degradation. Strength reduction is observed in the RC coupling beams at all stories



(a) Story drift ratio (b) Curvature ductility of RC beams

Figure 7. Seismic response of studied frames with RC coupling beams.

whereas yielding of the shear walls is measured at intermediate stories. Although the seismic design of general shear wall systems generally permits the plastic hinges at the only bases, seismic force demands of shear wall elements around the middle stories in a high-rise building could be larger than the design forces due to the effect of higher modes according to the existing studies on the dynamic behavior of high-rise structures (Blakeley et al., 1975; Panagiotou and Restrepo, 2009). As a result, plastic hinge is likely to occur at the shear wall located at middle stories. It can be found that the studied frames have relatively higher mass participation in second- and third-order modes than general low-rise structures.

The upper right plot in Fig. 8 indicate the displacement and overturning moment time-history responses. Total overturning moment (M_{ot}) is marked with black lines, and the overturning moment (Tl) by axial force applied to the shear wall is indicated with gray lines. The difference of these two overturning moments indicates the overturning moment resisted by the flexural moment capacity of each shear wall. This figure directly shows the time-history of the lateral load resistance by the frame action. The RC coupling beams of all stories suffer yielding and strength reduction during 6.8~9.1 seconds after ground shaking. Therefore, it can be found that as the studied frames show elastic behavior at below 6.8 seconds, the ratio of Tl to M_{ot} is large and the ratio significantly decreases after the failure of RC coupling beams. Also, for the story drift time-history, the drift starts to be increased with the initiation of the yielding of the RC coupling beams located at the 2nd floor. During 14 to 16 seconds where the maximum value of M_{ot} is measured, the total overturning moment of M_{ot} increases while the overturning moment of Tl keeps a nearly constant level. This means that the contribution of Tl on the total overturning moment M_{ot} is dependent on only the residual strength of the RC coupling beams whereas the flexural moment capacity of each RC shear wall becomes the main lateral-load carrying mecha-

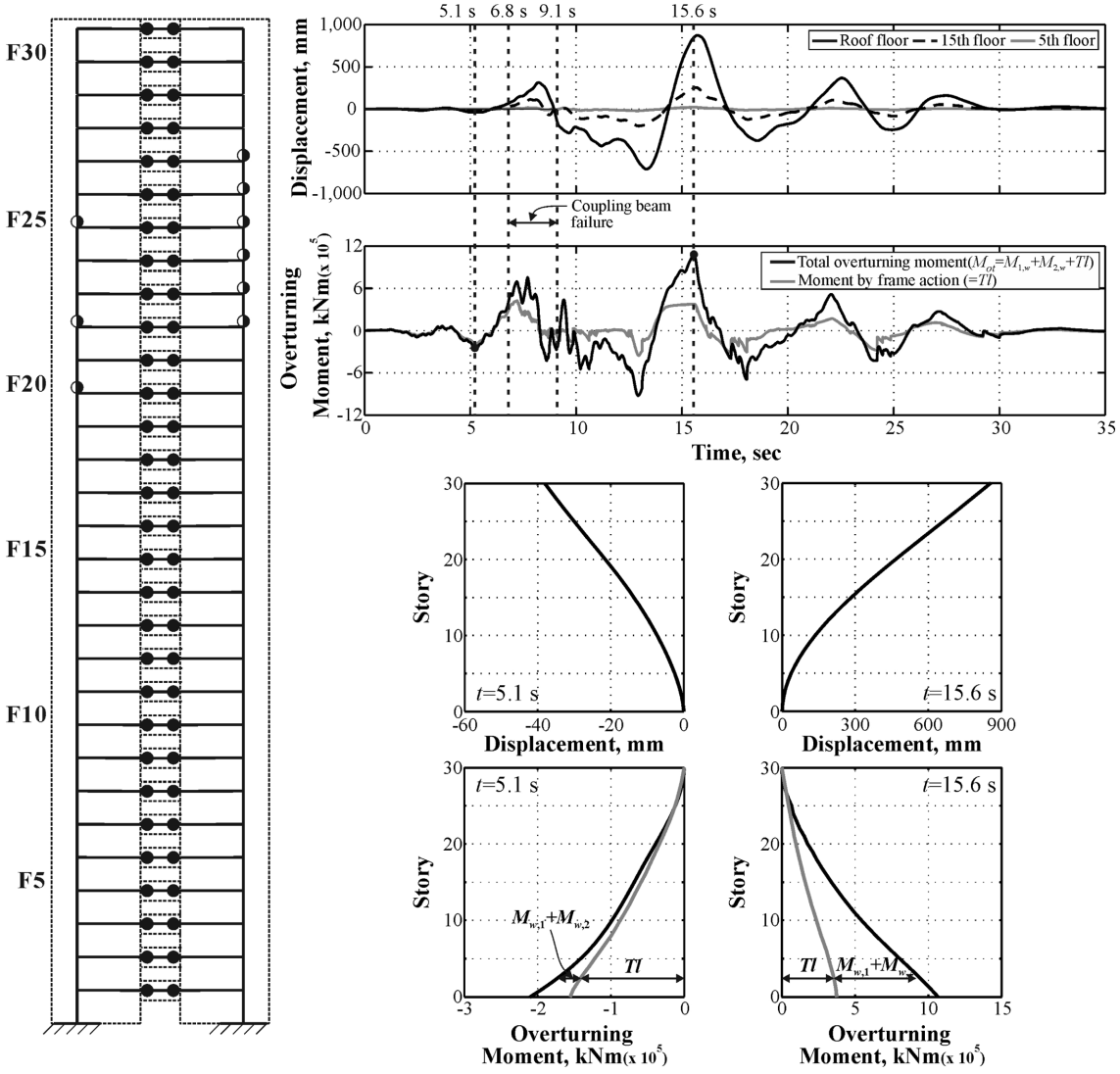


Figure 8. Summary of the analysis results of the studied frames under Kocaeli earthquake.

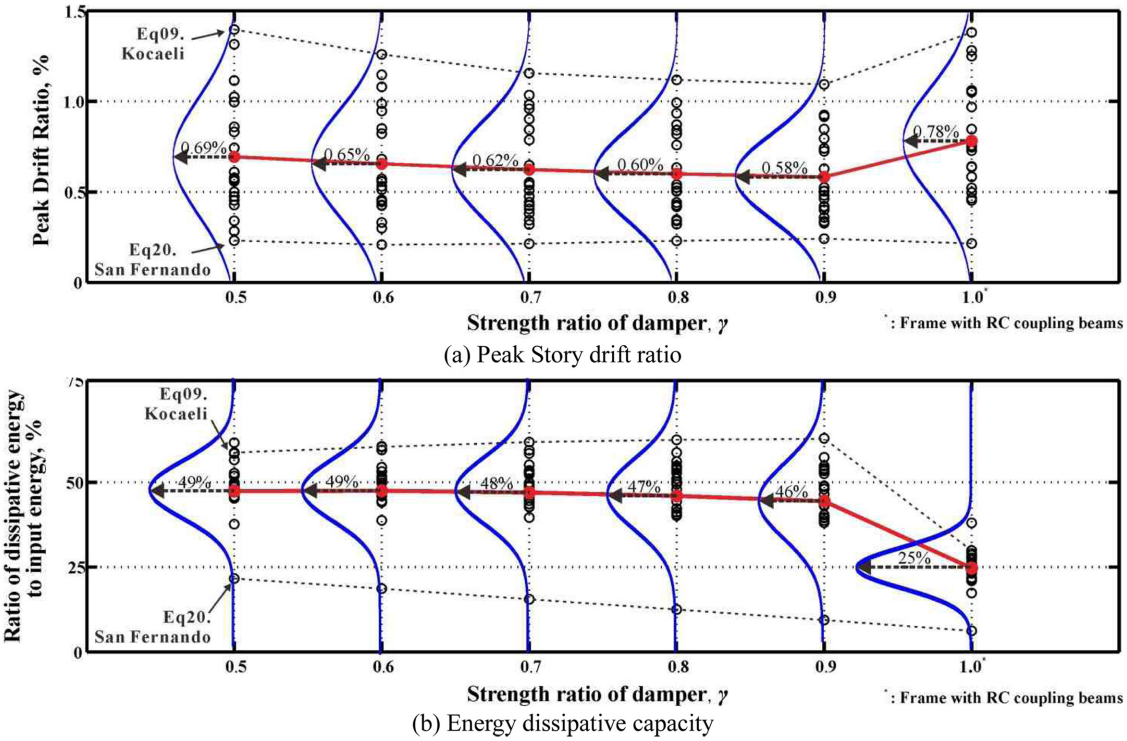
nism of the studied frame. The lower right graphs in Fig. 8 shows the comparison of instantaneous deformation shapes and story-specific distribution of M_{ot} and Tl before the yield of beams (t=5.1 second) and at the time of maximum overturning moment after failure of RC beams has occurred (t=15.6 second). The instantaneous deformation shapes at the two times all show the forms similar to the first-order mode. As the axial forces induced in the shear wall are, finally, equal to the sum of shear forces of each RC beam, the coupling effect by RC beams can be clearly identified when behaving as in the first-order mode. The ratios of Tl to Mot are 0.73 and 0.35 at t=5.1 and 15.6 seconds, respectively.

4.2. Seismic performance of a RC shear wall system with HEDDs

To investigate the seismic performance of the shear wall system with HEDDs, nonlinear time-history analyses are performed with changing γ (from 0.5 to 0.9 with spacing of 0.1) defined in the Eq. (3). For the time-history analysis of the damped structures, the same earthquake records used for the studied frames with RC coupling beams are utilized. The frictional HEDDs are assumed to be installed at all stories, and strength and stiffness are calculated by considering the cross section and yield moment of each RC coupling beam. Fig. 9(a) shows the maximum story drift ratios and average values according to the values of γ. The normal distribution curves obtained from the analysis results are also shown in the figure. The response of the studied frames with RC coupling beams (γ=1.0) is shown together in order to compare the effect of the HEDDs.

The damped structures show relatively small drift compared with studied frames with RC coupling beams. This is due to the fact that their energy dissipation capability has increased because of the plastic behavior of the HEDDs. It is also because the HEDDs show stable hysteretic behavior without strength degradation although they yields at strength smaller than the corresponding RC coupling beams. In addition, the hysteretic behavior of the HEDDs following the perfectly elasto-plastic hysteresis model dissipates energy more effectively than the RC coupling beams which are modeled by the Modified Takeda hysteretic elements. Due to this effect of dissipation energy, the average maximum story drift ratio has a tendency that it linearly increases as the values of γ become smaller.

The average maximum story drift ratio at γ=0.5 is 0.69% which is closest to 0.78% at γ=1. Among the 20 earthquake analysis results, the maximum story drift ratio is, respectively, 1.39% and 1.38% at γ=0.5 and γ=1 for the EQ09 Kocaeli record which generates the largest story drift ratio. It is interesting to find that similar deformation demands are measured although the strength of the HEDDs is a half of that of the RC coupling beams. For the EQ20 San Fernando record which generates the smallest story drift ratio, the story drift ratios of about 0.22% are observed regardless of the values of γ. This is due to the fact that very low level of story drift demands is required for the EQ20 San Fernando record. From the normal distribution curves of the maximum story drift ratios, as the values of γ become smaller, the distribution



(a) Peak Story drift ratio

(b) Energy dissipative capacity

Figure 9. Seismic response of studied frames with frictional HEDDs.

curves has a tendency to become gradually centered upon the average.

Fig. 9(b) shows the comparison of energy dissipation capability of the HEDDs with changing values of γ. In the figure, the ratios are defined as the normalized values of the energy dissipated by the RC coupling beams and HEDDs by the total input energy computed at the end of each analysis. While the structures with the frictional HEDDs dissipate 48% of input energy on average, the dissipation energy ratio of the studied frames with the RC coupling beams is 25%. The energy dissipation ratio has a tendency to somewhat increase as γ becomes smaller. However, the increasing rate is negligible and the frictional HEDDs dissipate amount of 49% of seismic input energy when the values of γ are equal to 0.5 and 0.6. Taking this into account, it is expected that the energy dissipation capacity of the frictional HEDDs would decrease if the values of γ are less than 0.5. The normal distribution curves of the energy ratios show that the RC shear wall system (γ=1) with the RC coupling beams presents the most crowded distribution while rather wide distribution is observed for the RC shear wall systems with the frictional HEDDs.

In terms of the relationship between the average energy dissipation rate and the average maximum story drift ratio, it can be found that a relatively small energy dissipation ratio is observed for the frictional HEDDs with high-yield strength (γ=0.9) whereas the systems employing the frictional HEDDs with relatively low-yield strength suffer large story drift ratio in order to obtain large energy dissipation. This increase in the story drift ratios is mostly due to the effect of the yield strength of the frictional HEDDs. Therefore, relatively larger yield strength of the frictional HEDDs can control the story drift response of the structure more effectively despite of the similar energy dissipation ratio.

Table 5 shows the comparison of the effects of frame action with changing values of γ when the EQ09 Kocaeli and EQ 20 San Fernando records have been applied. In the table the coupling effects are presented with the ratios of Tl to M_{ot}. When the EQ09 record is applied, the shear wall system with the frictional HEDDs has a tendency that the coupling effects become smaller as the values of γ decreases. For the shear wall system employing the friction HEDDs with the low-yield strength (γ=0.6), a ratio defining the coupling effects is 35.3%, which is similar value to the shear wall system with the RC coupling beams (γ=1). When the EQ20 San Fernando record is applied, the average ratios of 57.4% for the coupling effects are presented regardless of the values of γ. In addition, the maximum overturning moment M_{ot} during the EQ20 record is about 55% of that during the EQ09 record. This demonstrates that the effects of the frictional HEDDs on the lateral force resistance is not large for the earthquake where the small story drift demands are required.

Table 6 summarizes the values for the maximum rotational demands (MRDs) of the frictional HEDDs and the floor where the MRDs are measured. Values of maximum chord rotation of the RC coupling beams are also represented in the table. The MRDs is mostly measured at the frictional HEDDs located at top 2 floors. Because the frictional HEDDs are modeled with the same stiffness as that of RC beams, there is no large difference in the unique dynamic characteristics of the studied frames. Therefore, the studied frames with the frictional HEDDs show the maximum deformation around the roof floor as in studied frames with RC coupling beams. The maximum rotational demand increases with the decrease of the strength ratio of the frictional HEDDs. This tendency is noticeable in the analysis using earthquake records which generate larger deformation. The maximum rotational demand of the frictional HEDDs under the EQ09 record is approximately ten times greater than the value under the EQ20 record since the dissipated energy of the frictional HEDDs under the EQ20 record is relatively very small. The average values of the MRDs of the frictional HEDDs range between 0.026 and 0.035 with changing values of γ, whereas the maximum chord rotation of the RC coupling beams

Table 5. Comparison of Effect of Coupling by EQ09 and EQ20

Label	Strength ratio of damper, r	Total overturning moment, Mot (kNm)	Tl, (kNm)	Effect of coupling, Tl/Mot (%)
EQ09	0.5	910,955	278,687	30.6
	0.6	930,668	328,718	35.3
	0.7	954,281	375,386	39.3
	0.8	981,508	420,265	42.8
	0.9	1,011,090	461,950	45.7
	1.0	1,069,617	376,582	35.2
EQ20	0.5	413,073	237,567	57.5
	0.6	467,914	266,756	57.0
	0.7	516,112	296,153	57.4
	0.8	549,910	316,448	57.5
	0.9	575,195	334,094	58.1
	1.0	578,525	329,103	56.9

Table 6. Maximum rotational demand of RC coupling beam and HEDDs

Label	γ=0.5		γ=0.6		γ=0.7		γ=0.8		γ=0.9		γ=1.0	
	MCD	Floor	MCD	Floor	MCD	Floor	MCD	Floor	MCD	Floor	MCD	Floor
EQ01	0.052	30	0.050	30	0.048	30	0.046	29	0.045	29	0.064	26
EQ02	0.043	30	0.044	30	0.043	30	0.041	30	0.039	29	0.055	29
EQ03	0.043	31	0.041	31	0.039	31	0.037	30	0.035	30	0.042	30
EQ04	0.058	31	0.055	31	0.053	31	0.050	31	0.048	30	0.055	R
EQ05	0.027	29	0.024	28	0.022	27	0.020	26	0.019	25	0.026	R
EQ06	0.020	30	0.020	29	0.018	29	0.015	29	0.016	29	0.030	30
EQ07	0.023	31	0.023	31	0.022	31	0.020	30	0.019	30	0.027	30
EQ08	0.023	31	0.021	30	0.020	30	0.019	30	0.019	30	0.022	30
EQ09	**0.072**	**30**	**0.065**	**30**	**0.059**	**29**	**0.054**	**29**	**0.050**	**28**	**0.070**	**25**
EQ10	0.052	30	0.048	30	0.046	30	0.044	30	0.042	30	0.051	R
EQ11	0.067	30	0.058	30	0.048	29	0.040	29	0.033	29	0.064	26
EQ12	0.023	27	0.018	25	0.014	23	0.011	23	0.010	23	0.041	30
EQ13	0.029	30	0.028	30	0.027	30	0.026	30	0.024	30	0.037	R
EQ14	0.013	29	0.013	29	0.013	30	0.012	30	0.011	29	0.022	25
EQ15	0.037	31	0.034	30	0.032	30	0.031	30	0.030	30	0.041	R
EQ16	0.028	31	0.025	29	0.023	29	0.021	29	0.018	29	0.029	R
EQ17	0.029	30	0.026	30	0.023	30	0.021	30	0.020	30	0.039	27
EQ18	0.030	31	0.028	31	0.026	31	0.024	30	0.022	30	0.038	30
EQ19	0.015	28	0.013	27	0.012	26	0.010	28	0.009	27	0.027	28
EQ20	**0.007**	**24**	**0.005**	**23**	**0.004**	**23**	**0.004**	**23**	**0.004**	**3**	**0.010**	**3**
Mean	**0.035**		**0.032**		**0.030**		**0.027**		**0.026**		**0.039**	

Table 7. Maximum curvature ductility of shear wall

Label	γ=0.5		γ=0.6		γ=0.7		γ=0.8		γ=0.9		γ=1.0	
	MCD	Story	MCD	Story	MCD	Story	MCD	Story	MCD	Story	MCD	Story
EQ01	**5.6**	**19**	**4.6**	**19**	**3.9**	**19**	**3.8**	**19**	**3.6**	**19**	**6.7**	**19**
EQ02	**8.7**	**25**	**5.8**	**22**	**5.8**	**22**	**6.1**	**22**	**6.1**	**22**	**12.8**	**25**
EQ03	**12.4**	**25**	**9.4**	**25**	**7.0**	**25**	**6.6**	**25**	**6.2**	**25**	**15.1**	**25**
EQ04	**11.7**	**25**	**11.0**	**25**	**11.0**	**25**	**11.0**	**25**	**11.0**	**25**	**7.6**	**22**
EQ05	< 1	-	< 1	-	< 1	-	< 1	-	< 1	-	< 1	-
EQ06	< 1	-	< 1	-	< 1	-	< 1	-	< 1	-	< 1	-
EQ07	**6.0**	**25**	**5.3**	**25**	**4.6**	**25**	**4.3**	**25**	**4.3**	**25**	**6.8**	**25**
EQ08	**2.2**	**25**	**2.3**	**25**	**2.4**	**25**	**2.5**	**25**	**2.7**	**25**	**3.0**	**25**
EQ09	**2.8**	**25**	**3.0**	**25**	**3.1**	**25**	**3.3**	**25**	**3.5**	**25**	**3.7**	**25**
EQ10	**4.4**	**25**	**3.6**	**25**	**3.4**	**25**	**3.4**	**25**	**3.4**	**25**	**3.5**	**25**
EQ11	< 1	-	< 1	-	< 1	-	< 1	-	< 1	-	**1.5**	**25**
EQ12	< 1	-	< 1	-	< 1	-	< 1	-	< 1	-	< 1	-
EQ13	**2.5**	**25**	**2.4**	**25**	**2.3**	**25**	**2.4**	**25**	**2.6**	**25**	**5.5**	**25**
EQ14	**1.1**	**25**	< 1	-	< 1	-	< 1	-	< 1	-	**2.1**	**25**
EQ15	**2.0**	**25**	**1.8**	**25**	**1.9**	**25**	**2.1**	**25**	**2.3**	**25**	**3.1**	**25**
EQ16	< 1	-	< 1	-	< 1	-	< 1	-	< 1	-	**1.4**	**25**
EQ17	**2.2**	**25**	**1.8**	**25**	**1.7**	**25**	**1.6**	**25**	**1.6**	**25**	**1.3**	**25**
EQ18	**10.8**	**25**	**8.6**	**25**	**6.8**	**25**	**5.6**	**25**	**5.0**	**25**	**9.5**	**25**
EQ19	< 1	-	< 1	-	< 1	-	< 1	-	< 1	-	< 1	-
EQ20	< 1	-	< 1	-	< 1	-	< 1	-	< 1	-	< 1	-
Mean	**5.57**		**5.0**		**4.49**		**4.39**		**4.36**		**5.57**	

has the range of 0.01~0.07 and the average value is 0.039. Thus, a ratio of average rotation of each system is about 88%, 81%, 75%, 69% and 65%, respectively.

Table 7 shows the maximum curvature ductility demands (MCDs) of the RC shear walls excited by each earthquake record and the story where the MCDs are measured. When the EQ05, 06, 12, 19 and 20 earthquake records are applied, the RC shear walls are in elastic state. When the

yielding has occurred at the RC shear walls, however, the MCDs have mostly occurred at the shear wall located at the 25th floor. Although it has not been presented in this paper due to the restriction of space, the bases of the RC shear walls maintains elasticity in all analyses. It can be found from this that studied frames with the frictional HEDDs are critical to large higher-mode effects similar to the corresponding RC shear wall systems with the RC coupling beams. While the shear walls with RC coupling beams have the larger values of MCDs in most of analysis results, the MCDs of the shear wall with the frictional HEDDs show the irregular tendency depending of the earthquake records. Comparing the average MCD according to the values of γ, it increases as the values of γ decrease and the average MCD of 5.57 for the system with γ=0.5 is equal to that of the system with the RC coupling beams. From these, it can be confirmed that the RC shear wall systems employing the frictional HEDDs with γ=0.5 can presents similar seismic performance to the RC shear wall system with the RC coupling beams in terms of story drift demands.

5. Conclusion

This study carried out nonlinear time history analyses using 20 earthquake records scaled by the design acceleration spectrum in order to compare the seismic performance of high-rise shear wall structures with conventional RC coupling beams and frictional HEDDs with sufficient deformation capability. Non-linear dynamic analyses were performed using the variables γ which is the ratio of the yield strength of frictional HEDDs to that of RC coupling beams. The analysis results of each system were compared in terms of story drift ratios, energy dissipation capability, and ductility in order to find out the yield strength of frictional HEDDs showing the similar seismic response to the RC beam-connected shear wall systems. Results of this study are summarized as follows.

1) High-rise shear wall systems with conventional RC coupling beams designed according to the current code could suffer the destruction of RC coupling beams and in turn significantly decrease in the coupling effects under large deformation demand. The yield of shear walls in the high-rise buildings could occur at intermediate stories, not at the base, due to the higher mode effects.

2) In the shear wall systems with the frictional HEDDs, the average maximum drift ratios increase with the decrease of their yield strengths. However, the average maximum story drift ratio of the shear wall systems employing the frictional HEDDs with γ=0.5 is smaller than that of the corresponding shear wall system with the RC coupling beams by about 11.5%. This is due to the fact that the frictional HEDDs avoid strength and stiffness degradation reduction and present stable hysteresis.

3) Comparing the ratios of energy dissipated by the RC coupling beams and frictional HEDDs to input energy, the frictional HEDDs have double energy dissipating capacity to the RC coupling beams on average. However, there is little difference in energy dissipation capability even if the values of γ are smaller.

4) The average maximum rotational demand of the frictional HEDDs ranges 0.026 to 0.035 and the values increase with the decrease in the yield strength of the HEDDs. This tendency is more noticeable in earthquake records where larger deformation has occurred.

5) The shear wall system with the frictional HEDDs presents a tendency that the average maximum curvature ductility of the shear walls increases with the decreasing in their yield strength ratios. From this observation, the RC shear wall systems employing the frictional HEDDs with γ=0.5 can present similar seismic performance to the RC shear wall system with the RC coupling beams in terms of story drift demands.

References

ASCE. (2010). Minimum design loads for buildings and other structures, ASCE/SEI 7-10, Reston, VA, USA.

Blakeley, R. W. G., Cooney, R. C., and Megget, L. M. (1975). "Seismic shear loading at flexural capacity in cantilever wall structures." *Bulletin of the New Zealand National Society for Earthquake Engineering*, 8(4), pp. 278~290.

Boivin, Y. and Patrick, P. (2010). "Seismic performance of a 12-storey ductile concrete shear wall system designed according to the 2005 National building code of Canada and the 2004 Canadian Standard Association standard A23. 3." *Canadian Journal of Civil Engineering*, 37.1, pp. 1~16.

Carr, A. J. (2005) *User Manual for the 2: Dimensional Version Ruaumoko2D*. Department of Civil Engineering. University of Canterbury, Christchurch, New Zealand.

Chopra, A. K. (2001). *Dynamics of Structures*: *Theory and Applications to Earthquake Engineering*. Prentice-Hall: Upper, Saddle River, NJ, USA.

Christopoulos, C., Filiatrault, A., and Bertero, V. V. (2006). *Principles of passive supplemental damping and seismic isolation*. IUSS Press, Pavia, Italy.

Chung, H. S., Moon, B. W., Lee, S. K., Park, J. H., and Min, K. W. (2009). "Seismic performance of friction dampers using flexure of RC shear wall system." *The Structural Design of Tall and Special Buildings*, 18(7), pp. 807~822.

Collins, M. P. and Mitchell, D. (1987). *Prestressed concrete basics.* Canadian Prestressed Concrete Institute, Ottawa, Ont, CANADA.

Federal Emergency Management Agency (2000). *FEMA 356-Prestandard and Commentary for the Seismic Rehabilitation of Buildings.* Washington DC, USA.

Federal Emergency Management Agency (2009). *FEMA P695 Quantification of Building Seismic Performance Factors*. Washington, DC, USA.

Harries, K. A. (2000). "Ductility and deformability of coupling beams in reinforced concrete coupled walls." *Earthquake Spectra*, 16(4), pp. 775~800.

Harries, K. A., Mitchell, D., Redwood, R. G., and Cook, W. D. (1998). "Nonlinear seismic response predictions of walls coupled with steel and concrete beams." *Canadian Journal of Civil Engineering*, 25(5), pp. 803~818.

KBC. (2009). Korean Building Code, KBC2009, Architectural Institute of Korea.

Kim, H. J., Choi, K. S., Oh, S. H., and Kang, C. H. (2012). "Dissipative Coupling Beams used for RC Shear Walls Systems." *15WCEE*, Lisboa, Portugal, September.

Mander, J. B., Priestley, M. J., and Park, R. (1988). "Theoretical stress-strain model for confined concrete." *Journal of Structural Engineering*, 114(8), pp. 1804~1826.

Otani, S. (1974). *SAKE, a computer program for inelastic response of R/C frames to earthquakes*. Civil Engineering Studies, University of Illinois at Urban-champaign, Urbana, Ill., Report UILU-Eng-74-2029.

Panagiotou, M., and Restrepo, J. I. (2009). "Dual-plastic hinge design concept for reducing higher-mode effects on high-rise cantilever wall buildings." *Earthquake Engineering & Structural Dynamics*, 38(12), pp. 1359~1380.

Paulay, T. and Binney, J. R. (1974). "Diagonally Reinforced Coupling Beams of Shear Walls. *In* Shear in reinforced concrete" Publication No. SP-42, ACI, Detroit, Michigan, pp. 579~589.

Paulay, T. and Priestly, M. J. N. (1992). *Seismic design of reinforced concrete and masonry buildings*. John Wiley & Sons, New York, USA

Paulay, T. and Santhakumar, A. R. (1976). "Ductile Behavior of Coupled Shear Walls." *Journal of the Structural Division*, 102.1, pp. 93~108.

Priestley, M. J. N. and Kowalsky, M. J. (2000). "Direct displacement-based seismic design of concrete buildings." *New Zealand National Society for Earthquake Engineering*, Vol. 33, pp. 421~444.

Tremblay, R., Chen, L., and Tirca, L. (2014). "Enhancing the Seismic Performance of Multi-storey Buildings with a Modular Tied Braced Frame System with Added Energy Dissipating Devices." *International Journal of High-Rise Buildings*, 3(1), pp. 21~33.